Thermodynamic Analysis on the Mineralization of Trace Organic Contaminants with Oxidants in Advanced Oxidation Processes

ARTICLE *in* INDUSTRIAL & ENGINEERING CHEMISTRY RESEARCH · DECEMBER 2009

Impact Factor: 2.59 · DOI: 10.1021/ie900620n

Thermodynamic Analysis on the Mineralization of Trace Organic Contaminants with Oxidants in Advanced Oxidation Processes

Yuanhui Ji,[†] Zhuhong Yang,[†] Xiaoyan Ji,[‡] Xin Feng,[†] Wenjuan Huang,[†] Chang Liu,[†] Wei Li,[†] and Xiaohua Lu*,[†]

State Key Laboratory of Materials-Oriented Chemical Engineering, Nanjing University of Technology, Nanjing 210009, Jiangsu, People's Republic of China, and Division of Energy Engineering, Luleå University of Technology, SE-97187 Luleå, Sweden

There is a growing demand for the efficient treatment of organic polluted wastewaters by advanced oxidation processes (AOPs) which calls for the determination of the mineralization order of ease for the organic contaminants with oxidants. The mineralization abilities of organic contaminants in AOPs are investigated in this work. Photocatalytic experiments for three representative organic contaminants are carried out, and their corresponding reaction rates are determined experimentally. Meanwhile, molar Gibbs free energy changes $\Delta_r G_m^\circ$ for the reactions of 31 organic contaminants (10 chlorinated hydrocarbons, four brominated hydrocarbons, 11 aromatic hydrocarbons and their derivatives, three chloroacetic acid, and three chloroacetyl chloride) with oxidants of $^\bullet OH$, H_2O_2, $^\bullet O^-$, O_3, and O_2 are calculated, and the mineralization order of ease is determined theoretically on the basis of $\Delta_r G_m^\circ$. The agreement of the theoretical and experimental mineralization abilities for most of the organic contaminants investigated implies the reliability of the determination of the mineralization ability from the magnitude of $\Delta_r G_m^\circ$ for the mineralization of trace organic contaminants. Results also show that for most of the organic contaminants studied, the mineralization abilities are $^\bullet OH > H_2O_2 > {}^\bullet O^- > O_3 > O_2$, and the mineralization ability of the organic contaminants depends on not only the oxidants but also the structure and properties of the organic contaminants themselves, and the degradation reaction products.

1. Introduction

The widespread pollution of surface, ground, and drinking waters with toxic and hazardous organic contaminants demands an increasing effort toward the scientific and technological development for the cleanup of wastewaters. To mineralize the contaminants thoroughly, advanced oxidation processes (AOPs) have been used for the treatment of drinking water sources and for the remediation of contaminated waters.[1−4]

AOPs include TiO_2 and ultraviolet radiation (UV), ozone (O_3) and UV, the Fenton reagent (H_2O_2/Fe^{2+}), H_2O_2 and UV, O_3 with H_2O_2, high-frequency ultrasound waves, γ rays, and high-energy electrons, etc.[5−8] The feasibility of these processes has been verified experimentally.[2−5,8,9] In AOPs, hydroxyl radical ($^\bullet OH$) or other highly reactive radical species are generated and react rapidly with the organic contaminants in aqueous solutions.[10,11] Because of the diversity and the complexity of the contaminants in water, various AOPs are generally integrated to increase the degradation efficiency. To design the integrated AOPs, it is important to determine the mineralization order of ease for the organic contaminants with different oxidants.

Experimentally, the degradation rate constants are investigated to indicate the mineralization order of ease of organic contaminants,[9] and the larger the rate constants, the faster and easier the organic contaminants are mineralized. However, for some organic contaminants, the results of degradation order from different research groups are inconsistent. For example, for benzene and its derivatives, the degradation rate order is benzene > toluene > chlorobenzene in the work of Glaze and Kang,[12] while it is toluene > benzene > chlorobenzene in refs 13 and 14. Therefore, new reliable measurements and further theoretical analysis are needed.

On the other hand, as mentioned by Brezonik,[15] an empirical rate equation is used to fit the experimental data in order to obtain reaction rate constants. However, in most cases, the time related concentration data do not fit any rate expression exactly.[15] Consequently, it is desirable to measure the initial velocities and then obtain the rate constant. It is because, during this period, the product concentrations can be kept low and then the opportunities for side reactions are reduced.[15] Therefore, in this work, the photocatalytic experiments are performed to determine the degradation order of ease for three representative organic contaminants. The photocatalytic experiments are performed for 5 min in the same reactor with the same light intensity and similar initial concentrations of the organic contaminants.

Theoretically, previous research have shown that the reaction rate relates to activation energy and the driving force of a reaction, i.e., the Gibbs free energy change of reaction (ΔG_r).[16−18] In many AOPs, due to the addition of catalyst, the activation energy is decreased, and then the driving force (ΔG_r) becomes the main factor to control the reaction rate. In addition, most AOPs are performed at room temperature and 1 atm; i.e., $\Delta G_r = \Delta_r G^\circ$, and thus reaction rates can be reflected from the magnitude of $\Delta_r G^\circ$. This observation also has been verified in our previous work,[14] and the mineralization order of ease for eight organic contaminants with the oxidant of $^\bullet OH$ has been determined. However, in AOPs, many other oxidants may appear and react with the organic contaminants, and such theoretical study has not been performed yet. In this work, the mineralization order of aqueous organic contaminants with possible oxidants of $^\bullet OH$, H_2O_2, $^\bullet O^-$, O_3, and O_2 in AOPs will be determined from the calculated $\Delta_r G^\circ$, and the experimental

* To whom correspondence should be addressed. Tel.: +86-25-83588063. Fax: +86-25-83588063. E-mail: xhlu@njut.edu.cn.
[†] Nanjing University of Technology.
[‡] Luleå University of Technology.

10.1021/ie900620n CCC: $40.75
Published on Web 09/18/2009

results determined in our and other groups will be analyzed according to the calculated $\Delta_r G°$.

Therefore, in this work we will investigate the mineralization reactions for organic contaminants with oxidants in AOPs. The objectives are (a) to carry out photocatalytic experiments for representative organic contaminants, (b) to perform thermodynamic studies on the mineralization order of aqueous trace organic contaminants with possible oxidants of $^{\bullet}OH$, H_2O_2, $^{\bullet}O^-$, O_3, and O_2 in AOPs by calculating $\Delta_r G°_m$, and (c) to analyze the experiments results achieved by different groups according to $\Delta_r G°_m$ calculation results.

2. Experimental Section

2.1. Chemicals and Reagents. 1,2-Dichloroethane is chemically pure and purchased from Shanghai Lingfeng Chemical Reagent Co. Ltd., Shanghai, China. 1,2-Dichlorobenzene is chemically pure and purchased from Shanghai Reagent Plant No. 3, Shanghai, China. 1,1,2-Trichloroethylene is an analytical reagent and purchased from Shanghai Shiyi Chemical Reagent Co. Ltd., Shanghai, China. The TiO_2 photocatalyst P-25, with the specific surface area of 50 $m^2 \cdot g^{-1}$, is purchased from Degussa Co., Dusseldorf, Germany, and the mass ratio of the anatase to rutile is about 4.

2.2. Photocatalytic Degradation Reaction and Experimental Procedure. The photocatalytic degradation reaction is performed in a batch reactor XPA-II Model photochemical reactor (Nanjing XuJiang Co.). The volume of the reactor is 1.0 L, a medium-pressure Hg lamp of 300 W is put in the middle, and recycled water is used for cooling. The reactant solution is stirred by a magnetic stirrer to keep the catalyst suspended in the solutions. The catalyst P-25 and H_2O are dispersed by ultrasonic concussion for 10 min before they are put into the reactor with the organic solution. Then the magnetic stirrer and ultraviolet lamp are turned on, and air flows into the reactor with the flow rate of 200 $mL \cdot min^{-1}$. The adaptometer begins timing when the catalyst and the aqueous solutions are mixed adequately, and the sample volume for analysis is 15 mL. After the analysis sample is taken out, the catalyst is removed using filtration membrane with 0.22 μm.

2.3. Analytical Equipment and Methods. SP-6890 Model gas chromatograph (Shandong Lunan Ruihong Chemical Instrument Co. Ltd.) is used to measure the concentrations of 1,2-dichlorobenzene. The quartz capillary chromatographic column is 0.32 mm × 30 m; the fixed phase is SE-54. The detection conditions are that the temperature of the boiling room and measuring room is 210 °C; the initial temperature is 150 °C. The concentrations of 1,2-dichloroethane and 1,1,2-trichloroethylene are determined by measuring the concentrations of the product Cl^- with ion selective electrodes. A SCHOTT-GERÄTE pH meter (Model CG0841, Mainz, Germany) is used to monitor the potential of the cell with a resolution of ±0.1 mV.

3. Thermodynamic Calculation on Molar Gibbs Energy Change of Reaction $\Delta_r G°$

The mineralization order of ease for the organic contaminants with different oxidants is important in designing integration AOPs. Since it is reliable to determine the mineralization order of ease from the magnitude of $\Delta_r G°$,[14] $\Delta_r G°$ for the reactions of 31 common aqueous organic contaminants with possible oxidants of $^{\bullet}OH$, H_2O_2, $^{\bullet}O^-$, O_3, and O_2 is calculated, and the mineralization order of ease is determined on the basis of $\Delta_r G°$. To make the $\Delta_r G°$ comparable, all the reactions are studied with the produced carbon dioxide as 1 mol ($\Delta_r G°_m$).

Table 1. Organic Contaminants Degradation Rate

organic contaminants		C_0 ($mg \cdot L^{-1}$)	r_0 ($mg \cdot L^{-1} \cdot min^{-1}$)
chlorinated hydrocarbons	1,1,2-trichloroethylene	110	2.78
	dichloromethane[14]	132	2.52
	chloroform[14]	120	2.07
	1,1-dichloroethane	110	1.01
	tetrachlorocarbon[14]	80	0.11
benzene and its derivatives	1,2-xylene[14]	100	2.56
	toluene[14]	90	1.57
	benzene[14]	90	1.56
	chlorobenzene[14]	100	1.47
	1,2-dichlorobenzene	80	1.29
	phenol[14]	100	1.17

The aqueous organic contaminants investigated in this work are classified into five groups by a clustering analysis method according to the structure of organics, and the corresponding standard molar Gibbs energies of formation of aqueous organic contaminants $\Delta_f G°_m$(aq) at 298.15 K is taken from refs 14 and 19 and listed in Table S1 of the Supporting Information. The evaluated and reliable $\Delta_f G°_m$(aq) for liquid water and that for oxidants, CO_2, halogen ions, and inorganic acid ions in aqueous solutions at 298.15 K are taken from refs 20−23 and listed in Table S2 of the Supporting Information.

The calculation of $\Delta_r G°_m$ for the reaction of chloroform ($CHCl_3$) with the oxidant of $^{\bullet}OH$ is shown as an example to describe the calculation in detail.

The reaction equation of $CHCl_3$ with $^{\bullet}OH$ can be written as

$$CHCl_3(aq) + 2^{\bullet}OH(aq) \rightleftharpoons CO_2(aq) + 3H^+(aq) + 3Cl^-(aq) \quad (1)$$

For reaction 1, $\Delta_r G°_m$ can be calculated as

$$\Delta_r G°_m = \sum_B \nu_B \Delta_f G°_m(B) \quad (2)$$

$$= \Delta_f G°_m(CO_2(aq)) + 3\Delta_f G°_m(H^+(aq)) + 3\Delta_f G°_m(Cl^-(aq)) - \Delta_f G°_m(CHCl_3(aq)) - 2\Delta_f G°_m(^{\bullet}OH(aq))$$

$$= -732.8884 \text{ kJ/mol}$$

$\Delta_r G°_m$ for the reactions of $CHCl_3$ with other oxidants and other organic contaminants with five oxidants can be calculated with the same method. The reaction equations and the corresponding $\Delta_r G°_m$ calculated in this work are listed in Tables S3−S7 in the Supporting Information.

4. Results and Discussion

4.1. Experimental Results. The mineralization reaction rates with Degussa P-25 as the photocatalyst for the organic contaminants of 1,1,2-trichloroethylene, 1,1-dichloroethane, and 1,2-dichlorobenzene are measured in this work and listed in Table 1 together with our previous photocatalytic experimental results.[14] In Table 1, C_0 is the initial concentration of the investigated organic contaminants and r_0 is the average degradation rate of the organic contaminants in the initial 5 min and is calculated by $(C_0 - C_t)/t$, where C_t is the concentration of the investigated organic contaminants at a certain time t. The values of r_0 reveal the degradation ability of organic contaminants. Since the r_0 listed in Table 1 is sequenced from large to small for each group, the corresponding mineralization ability of the organic contaminants in each group is from high to low.

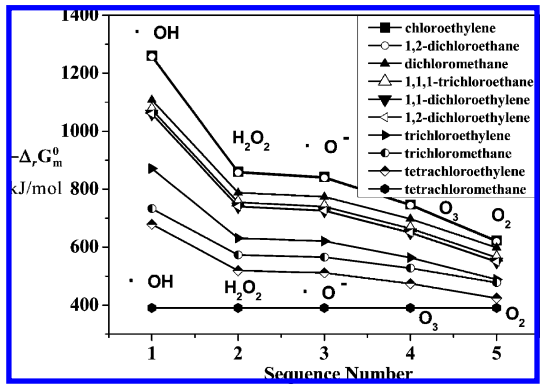

Figure 1. $\Delta_r G_m^\circ$ for the reactions of chlorinated hydrocarbons with five oxidants.

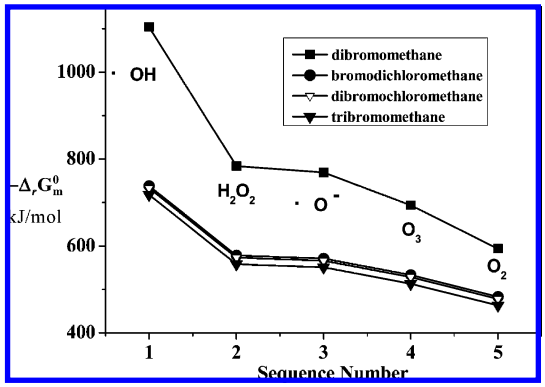

Figure 2. $\Delta_r G_m^\circ$ for the reactions of brominated hydrocarbons with five oxidants.

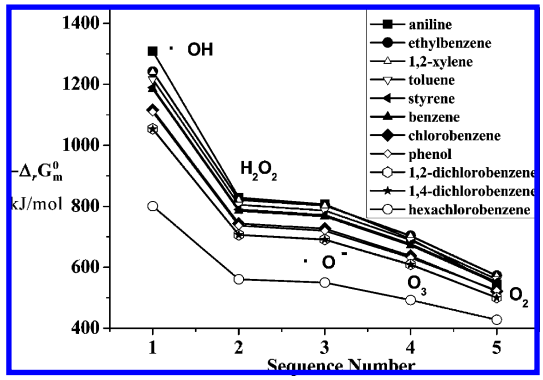

Figure 3. $\Delta_r G_m^\circ$ for reactions of aromatic hydrocarbons and their derivatives with five oxidants.

4.2. Comparison and Discussions on the Mineralization Order of Ease. The determination of the mineralization order of ease for the organic contaminants with oxidants is vital for the efficient design of integration AOPs. Mineralization rates have been measured experimentally to determine the mineralization order of ease. $\Delta_r G_m^\circ$ for the reaction of the common organic contaminants in water with five possible oxidants is calculated to determine the mineralization order of ease, and the smaller the $\Delta_r G_m^\circ$, the easier the mineralization of organic contaminants. The calculation results are shown in Figures 1−5. Since the $\Delta_r G_m^\circ$ is sequenced from small to large, the sequence number also represents the mineralization order of ease of aqueous organic contaminants. For almost all the organic contaminants investigated in this work, $\Delta_r G_m^\circ$ is negative, which means that essentially all organic contaminants are thermodynamically

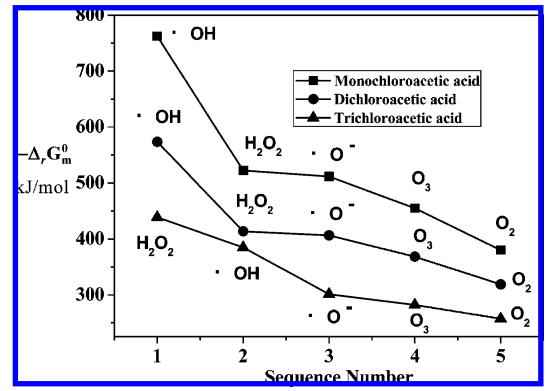

Figure 4. $\Delta_r G_m^\circ$ for the reactions of chloroacetic acids with five oxidants.

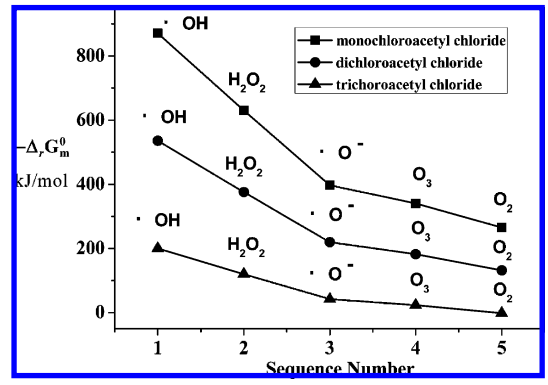

Figure 5. $\Delta_r G_m^\circ$ for the reactions of chloroacetyl chloride with five oxidants.

Table 2. Experimental Investigations of the Mineralization Ability for Chloromethanes

	sequence	method	ref
1	$CH_2Cl_2 > CHCl_3 \gg CCl_4$	TiO_2 photocatalysis	Ollis[9]
2	$CHCl_3 > CH_2Cl_2 > CCl_4$	H_2O_2/UV	Sundstrom et al.[24]
3	$CH_2Cl_2 > CHCl_3 > CCl_4$	TiO_2 photocatalysis	Sabin et al.[2]
4	$CH_2Cl_2 > CHCl_3 > CCl_4$	TiO_2 photocatalysis	Ji et al.[14]

unstable with respect to oxidation. This observation agrees with the view of Glaze and Kang.[12]

4.2.1. Chlorinated Hydrocarbons. Figure 1 shows the mineralization order of the five oxidants for the mineralization of 10 chlorinated hydrocarbons. As shown in Figure 1, for the mineralization of chlorinated hydrocarbons, the order is $^{\bullet}OH > H_2O_2 > {}^{\bullet}O^- > O_3 > O_2$.

The mineralization ease order of chloromethanes is $CH_2Cl_2 > CHCl_3 > CCl_4$, and the mineralization ability of the alkenes follows chloroethylene > 1,1-dichloroethylene ≈ 1,2-dichloroethylene > trichloroethylene > tetrachloroethylene. These results reveal a lower degradation ability with more C−H bonds being replaced by C−Cl bonds in alkanes and alkenes, and this observation agrees with the work of Sabin et al.[2]

The mineralization ability order of chloromethanes has been investigated experimentally[2,5,9,14,24] and is summarized in Table 2. In the TiO_2 photocatalysis investigated by Sabin et al.,[2] the first-order rate equation is used, while in the TiO_2 photocatalysis investigated by Ollis,[9] for all 12 halogenated hydrocarbons examined, the initial rate of reaction is proportional to the coverage, θ_x: rate $= k\theta_x$, where θ_x is given by a Langmuir isotherm, $\theta_x = (KC)/(1 + KC)$, where C is the solution reactant concentration and K is the apparent binding constant of the intermediate on the illuminated catalyst. For the investigations of trace organic contaminants in aqueous solutions, the con-

centration C of the organic contaminants is very low, so the expression of the coverage could be simplified as $\theta_x = (KC)/(1 + KC) \approx KC$. Therefore, the degradation rate could be simplified as rate $\approx kKC$, which shows the degradation order at low concentrations is characterized by the parameter product kK. Table 2 shows that the mineralization orders from Sabin et al.[2] and Ollis[9] are consistent. The mineralization ease order of chloromethanes from $\Delta_r G_m^\circ$ calculation agrees with the experimental results by Sabin et al.,[2] Ollis,[9] and Ji et al.[14]

In addition, the mineralization ability order of the alkenes obtained from $\Delta_r G_m^\circ$ in this work is consistent with experimental results from Ollis,[9] Glaze and Kang,[12] and Sabin et al.[2] Meanwhile, the mineralization ability of 1,1,1-trichloroethane is larger than trichloroethylene, which also agrees with the experimental results of ref 5. These agreements verify the reliability of the determination of the mineralization ability from the magnitude of $\Delta_r G_m^\circ$ calculated in this work.

However, according to the experimental results in our previous work[14] and those by Ollis[9] and Sabin et al.,[2] the degradation ability of trichloroethylene is stronger than dichloromethane, and the experimental results in this work and those by Haarstrick et al.[25] show that the mineralization ability of trichloroethylene is higher than that of dichloroethane, which disagrees with the results obtained from $\Delta_r G_m^\circ$. This may attribute to the yield of the unstable intermediates, such as dichloroacetaldehyde and dichloroacetic acid in the degradation experiments of trichloroethylene[9,26,27] and the higher mineralization rate of the intermediate dichloroacetaldehyde compared to that of trichloroethylene, dichloromethane, and dichloroethane.[28]

4.2.2. Brominated Hydrocarbons. Figure 2 shows the calculated $\Delta_r G_m^\circ$ for the mineralization of brominated hydrocarbons with oxidants. According to Figure 2, the mineralization ease order is dibromomethane > bromodichloromethane > dibromochloromethane > tribromomethane and the mineralization ability of the oxidants follows the order of $^\bullet OH > H_2O_2 > {}^\bullet O^- > O_3 > O_2$.

The mineralization order of brominated hydrocarbons can be determined from experimental results. In the work by Ollis,[9] the intrinsic rate constant shows the degradation order of $CHBr_3 > CH_2Br_2$ while the binding constant shows the order of $CH_2Br_2 > CHBr_3$. In the work by Nguyen and Ollis,[29] it shows that the order of intrinsic reactivity is $CHBr_3 > CH_2Br_2$ from k_R values, while it is $CH_2Br_2 > CHBr_3$ from the products of $k_R K_R$, where k_R and K_R are the intrinsic rate constant and the binding constant, respectively. However, the degradation order at low concentrations should be characterized by the parameter product $k_R K_R$.[9,29] So the experimental mineralization order for trace brominated methanes should be $CH_2Br_2 > CHBr_3$, which shows our calculation results for trace brominated hydrocarbons agree with the experimental results.

4.2.3. Aromatic Hydrocarbons and Their Derivatives. $\Delta_r G_m^\circ$ for the reactions of aromatic hydrocarbons and their derivatives with oxidants is shown in Figure 3. The mineralization ability of the oxidants follows $^\bullet OH > H_2O_2 > {}^\bullet O^- > O_3 > O_2$. If $^\bullet OH$, H_2O_2, and $^\bullet O^-$ are used as oxidants, the mineralization order for aromatic contaminants is aniline > ethylbenzene $\approx$ 1,2-xylene > toluene > styrene $\approx$ benzene > chlorobenzene > phenol > 1,2-dichlorobenzene $\approx$ 1,4-dichlorobenzene > hexachlorobenzene. If O_3 is used as oxidant, the mineralization order follows ethylbenzene $\approx$ 1,2-xylene > aniline > toluene > styrene $\approx$ benzene > chlorobenzene > phenol > 1,2-dichlorobenzene $\approx$ 1,4-dichlorobenzene > hexachlorobenzene. If O_2 is used as oxidant, the mineralization order is ethylbenzene $\approx$ 1,2-xylene > toluene > styrene > benzene > aniline > phenol > chlorobenzene > 1,2-dichlorobenzene $\approx$ 1,4-dichlorobenzene > hexachlorobenzene.

The mineralization order for benzene and its derivatives has been determined experimentally. In the review in ref 5, the efficiency of the H_2O_2/UV process with a variety of aromatic compounds was investigated in batch and flow reactors equipped with low-pressure Hg lamps. And the mineralization order is toluene > benzene > phenol > chlorobenzene. In the summary of Glaze and Kang,[12] it is benzene (pulse radiolysis, pH = 7) > toluene (pulse radiolysis, pH = 7) > chlorobenzene (γ radiolysis, pH = 9). The experimental results by TiO_2 photocatalysis in this work show that it is 1,2-xylene > toluene > benzene > chlorobenzene > 1,2-dichlorobenzene > phenol. Therefore, the order of these systems obtained from $\Delta_r G_m^\circ$ in this work is the same as the experimental results obtained in our work and those by Legrini et al.[5] except for phenol. According to the degradation details of phenol from refs 30 and 31 for the degradation of phenol, some ring compounds (e.g., 1,2,4-trihydroxybenze, 1,4-benzoquinone, catechol, and hydroquinone) are produced as the stable intermediates, which may bring interventions and affect the rates for the degradation of phenol.

4.2.4. Chloroacetic Acid. Haloacetic acids are known as disinfection byproducts, and their total level in drinking water cannot exceed the regulatory standards set, e.g., 60 $\mu g \cdot L^{-1}$ in the United States.[26] Figure 4 shows the ease order for the mineralization reaction is monochloroacetic acid (MCA) > dichloroacetic acid (DCA) > trichloroacetic acid (TCA). While the experimental results by Ollis[9] and Halmann[28] show that the degradation order is DCA > MCA > TCA. According to the degradation details of DCA from ref 34 during the degradation process of DCA, phosgene ($COCl_2$) is produced. According to the research results investigated by Ollis et al.,[31] the degradation rates of phosgene ($COCl_2$) and DCA follow the order $COCl_2 \gg$ DCA; the rapid consumption of the intermediate $COCl_2$ will accelerate the degradation reaction of the DCA. According to the detailed experimental results by Czili and Horváth,[32] the rate of disappearance of MCA and that of chloride formation from MCA are the same within the experimental error and the carbon containing intermediates are not detected. This may give an explanation why the degradation of DCA is higher than that of MCA. According to the photocatalytic degradation results of DCA over various bare and silver-deposited Degussa P-25 TiO_2 particles under aerobic conditions, the Cl^- formation rate of DCA is over two times that of MCA, which agrees with the above analysis results. Moreover, the stoichiometric decrease of total organic carbon in the liquid phase indicates that there is no significant amount of intermediate containing carbon atom(s) during the photodegradation of TCA.

As shown in Figure 4, for the degradation of MCA and DCA, the mineralization ability of the oxidants follows $^\bullet OH > H_2O_2 > {}^\bullet O^- > O_3 > O_2$, while, for the mineralization of trichloroacetic acid, it follows $H_2O_2 > {}^\bullet OH > {}^\bullet O^- > O_3 > O_2$. The low magnitude of $\Delta_r G_m^\circ$ for the reaction of trichloroacetic acid explains why trichloroacetic acid is nearly nonreactive in the TiO_2 photocatalytic experiment.[9]

In the review of ref 5 only according to the standard oxidation potential (volt) of the oxidants, it is stated that the oxidation potential of the oxidants follows the order of $^\bullet OH > O_3 > H_2O_2$. The calculation results indicate that the volts of the oxidation potential may not always represent the mineralization ability of the organic contaminants. The mineralization ability of the organic contaminants depends on not only oxidants but also

the structure and properties of the organic contaminants themselves and the mineralization products.

4.2.5. Chloroacetyl Chloride. $\Delta_r G_m^\circ$ for the reactions of chloroacetyl chloride with oxidants is shown in Figure 5. $\Delta_r G_m^\circ$ of trichloroethylene is lower than that of dichloroacetyl chloride, meaning an easier mineralization of trichloroethylene. This agrees with the statement that dichloroacetyl chloride is significantly less degradable than trichloroethylene.[26] Moreover, the positive $\Delta_r G_m^\circ$ for the mineralization of trichloroacetyl chloride with the oxidant of O_2 means that trichloroacetyl chloride cannot be decomposed by the oxidation reaction with O_2 as oxidant. The low magnitude of $\Delta_r G_m^\circ$ for all chloroacetyl chlorides implies that it is difficult to mineralize the chloroacetyl chlorides completely with mineral acids, carbon dioxide, and water as final products by AOPs.

As shown in Figure 5, the mineralization order of ease is monochloroacetyl chloride > dichloroacetyl chloride > trichloroacetyl chloride. For the mineralization of chloroacetyl chlorides, the oxidation ability of the oxidants follows $^{\bullet}OH > H_2O_2 > {}^{\bullet}O^- > O_3 > O_2$.

5. Conclusions

The mineralization abilities of organic contaminants in AOPs are investigated in this work. Photocatalytic experiments for three representative organic contaminants are carried out, and their corresponding reaction rates are determined experimentally. Meanwhile, molar Gibbs free energy changes $\Delta_r G_m^\circ$ for the reactions of 31 organic contaminants (10 chlorinated hydrocarbons, four brominated hydrocarbons, 11 aromatic hydrocarbons and their derivatives, three chloroacetic acid, and three chloroacetyl chloride) with oxidants of $^{\bullet}OH$, H_2O_2, $^{\bullet}O^-$, O_3, and O_2 are calculated, and the mineralization order of ease is determined theoretically on the basis of $\Delta_r G_m^\circ$. The agreement of the theoretical and experimental mineralization abilities for most of the organic contaminants investigated implies the reliability of the determination of the mineralization ability from the magnitude of $\Delta_r G_m^\circ$ for the mineralization of trace organic contaminants. Results also show that, for most of the organic contaminants studied, the oxidation abilities are $^{\bullet}OH > H_2O_2 > {}^{\bullet}O^- > O_3 > O_2$, and the mineralization ability of the organic contaminants depends on not only oxidants but also the structure and properties of the organic contaminants themselves and the degradation reaction products.

Acknowledgment

This work was supported by the Chinese National Key Technology Research and Development Program (Grant Nos. 2006BAB09B02, 2006AA03Z455, and 2006BAE03B7-2), National Basic Research Program of China (Grant No. 2009CB226103), the National Natural Science Foundation of China (Grant Nos. 20676062, 20731160614, 20736002, B061101, B060105, 20706029, and 20706028), NSFC-RGC (Grant No. 20731160614), the Natural Science Foundation of the Jiangsu Higher Education Institutions of China (Grant No. 08KJB530003), and Program for Changjiang Scholars and Innovative Research Team in University (Grant No. IRT0732). The authors are thankful to the anonymous reviewers for their time and helpful and revelatory comments and suggestions.

Supporting Information Available: Standard molar Gibbs energies of formation of aqueous organic contaminants, liquid water, and those for oxidants, CO_2, halogen ions, and inorganic acid ions in aqueous solutions ($\Delta_f G_m^\circ$(aq)) (Tables S1 and S2) and mineralization reaction equations for the organic contaminants with five oxidants and the calculated molar Gibbs energy change of reaction $\Delta_r G_m^\circ$ (Tables S3−S7). This material is available free of charge via the Internet at http://pubs.acs.org.

Literature Cited

(1) Benitez, F. J.; Beltran-Heredia, J.; Acero, J. L.; Rubio, F. J. Contribution of free radicals to chlorophenols decomposition by several advanced oxidation processes. *Chemosphere* **2000**, *41*, 1271–1277.

(2) Sabin, F.; Türk, T.; Vogler, A. Photo-oxidation of organic compound in the presence of titanium dioxide: Determination of the efficiency. *J. Photochem. Photobiol., A* **1992**, *63*, 99–106.

(3) Shemer, H.; Sharpless, C. M.; Elovitz, M. S.; Linden, K. G. Relative rate constants of contaminant candidate list pesticides with hydroxyl radicals. *Environ. Sci. Technol.* **2006**, *40*, 4460–4466.

(4) Zhang, H. C.; Lemley, A. T. Reaction mechanism and kinetic modeling of DEET degradation by flow-through anodic fenton treatment (FAFT). *Environ. Sci. Technol.* **2006**, *40*, 4488–4494.

(5) Legrini, O.; Oliveros, E.; Braun, A. M. Photochemical processes for water treatment. *Chem. Rev.* **1993**, *93*, 671–698.

(6) Priya, M. H.; Madras, G. Kinetics of photocatalytic degradation of chlorophenol, nitrophenol, and their mixtures. *Ind. Eng. Chem. Res.* **2006**, *45*, 482–486.

(7) Gu, L.; Zhang, X.; Lei, L. Degradation of aqueous p-nitrophenol by ozonation integrated with activated carbon. *Ind. Eng. Chem. Res.* **2008**, *47*, 6809–6815.

(8) Ahmed, B.; Mohamed, H.; Limen, E.; Nasr, B. Degradation and mineralization of organic pollutants contained in actual pulp and paper mill wastewaters by a UV/H_2O_2 process. *Ind. Eng. Chem. Res.* **2009**, *48*, 3370–3379.

(9) Ollis, D. F. Contaminant degradation in water. *Environ. Sci. Technol.* **1985**, *19*, 480–484.

(10) Beltrán, F. J.; Rivas, J.; Álvarez, P. M.; Alonso, M. A.; Acedo, B. A kinetic model for advanced oxidation processes of aromatic hydrocarbons in water: Application to phenanthrene and nitrobenzene. *Ind. Eng. Chem. Res.* **1999**, *38*, 4189–4199.

(11) Alberici, R. M.; Jardim, W. F. Photocatalytic degradation of phenol and chlorinated phenols using Ag-TiO_2 in a slurry reactor. *Water Res.* **1994**, *28*, 1845–1849.

(12) Glaze, W. H.; Kang, J. W. Advanced oxidation processes. Description of a kinetic model for the oxidation of hazardous materials in aqueous media with ozone and hydrogen peroxide in a semibatch reactor. *Ind. Eng. Chem. Res.* **1989**, *28*, 1573–1580.

(13) Sundstrom, D. W.; Klei, H. E. *Destruction of hazardous compounds by ultraviolet catalyzed oxidation with hydrogen peroxide*; NTIS Publication No. PB87-149357; National Technical Information Service: Springfield, VA, 1986.

(14) Ji, Y. H.; Yang, Z. H.; Ji, X. Y.; Huang, W. J.; Feng, X.; Liu, C.; Lu, L. H.; Lu, X. H. Thermodynamic study on the reactivity of trace organic contaminant with the hydroxyl radicals in waters by advanced oxidation processes. *Fluid Phase Equilib.* **2009**, *277*, 15–19.

(15) Brezonik, P. L. *Chemical kinetics and process dynamics in aquatic systems*; CRC Press: Boca Raton, FL, 1994.

(16) Parmon, V.; Emeline, A. V.; Serpone, N. Glossary of terms in photocatalysis and radiocatalysis. *Int. J. Photoenergy* **2002**, *4*, 91–131.

(17) Garfinkle, M. The thermodynamic natural path in chemical reaction kinetics. *Discrete Dyn. Nat. Soc.* **2000**, *4*, 145–164.

(18) Vuddagiri, S. R.; Hall, K. R.; Eubank, P. T. Dynamic modeling of reaction pathways on the Gibbs energy surface. *Ind. Eng. Chem. Res.* **2000**, *39*, 508–517.

(19) Helgeson, H. C. Calculation of the thermodynamic properties and relative stabilities of aqueous acetic and chloroacetic acids, acetate and chloroacetates, and acetyl and chloroacetyl chlorides at high and low temperatures and pressures. *Appl. Geochem.* **1992**, *7*, 291–308.

(20) Buxton, G. V.; Greenstock, C. L.; Helman, W. P.; Ross, A. B. Critical review of rate constants for reactions of hydrated electrons, hydrogen atoms and hydroxyl radicals ($^{\bullet}OH/{}^{\bullet}O^-$) in aqueous solution. *J. Phys. Chem. Ref. Data* **1988**, *17*, 513–886.

(21) Wagman, D. D.; Evans, W. H.; Parker, V. B.; Schumm, R. H.; Halow, I.; Bailey, S. M.; Churney, K. L.; Nuttall, R. L. The NBS tables of chemical thermodynamic properties. Selected values for inorganic and C_1 and C_2 organic substances in SI units. *J. Phys. Chem. Ref. Data* **1982**, *11* (Suppl. 2), 1–407.

(22) Alberty, R. A. Standard transformed formation of carbon dioxide in aqueous solutions at specified pH. *J. Phys. Chem.* **1995**, *99*, 11028–11034.

(23) Alberty, R. A. Apparent equilibrium constants and standard transformed Gibbs energies of biochemical reactions involving carbon dioxide. *Arch. Biochem. Biophys.* **1997**, *348* (1), 116–124.

(24) Sundstrom, D. W.; Klei, H. E.; Nalette, T. A.; Reidy, D. J.; Weir, B. A. Destruction of halogenated aliphatics by ultraviolet catalyzed oxidation with hydrogen peroxide. *Hazard. Waste Hazard. Mater.* **1986**, *3* (1), 101–110.

(25) Haarstrick, A.; Kut, O. M.; Heinzle, E. TiO_2-assisted degradation of environmentally relevant organic compounds in wastewater using a novel fluidized bed photoreactor. *Environ. Sci. Technol.* **1996**, *30*, 817–824.

(26) Li, K.; Stefan, M. I.; Crittenden, J. C. UV photolysis of trichloroethylene: product study and kinetic modeling. *Environ. Sci. Technol.* **2004**, *38*, 6685–6693.

(27) Glaze, W. H.; Kenneke, J. F.; Ferry, J. L. Chlorinated byproducts from the TiO_2- mediated photodegradation of trichloroethylene and tetrachloroethylene in water. *Environ. Sci. Technol.* **1993**, *27*, 177–184.

(28) Halmann M. M. *Photodegradation of water pollutants.*; CRC Press; New York, 1995, 114−115.

(29) Nguyen, T.; Ollis, D. F. Complete heterogeneously photocatalyzed transformation of 1,1- and 1,2-dibromoethane to CO_2 and HBr. *J. Phys. Chem.* **1984**, *88*, 3386–3388.

(30) Zazo, J. A.; Casas, J. A.; Mohedano, A. F.; Gilarranz, M. A.; Rodríguez, J. J. Chemical pathway and kinetics of phenol oxidation by Fenton's reagent. *Environ. Sci. Technol.* **2005**, *39*, 9295–9302.

(31) Ortiz-Gomez, A.; Serrano-Rosales, B.; Salaices, M.; de Lasa, H. Photocatalytic oxidation of phenol: reaction network, kinetic modeling, and parameter estimation. *Ind. Eng. Chem. Res.* **2007**, *46*, 7394–7409.

(32) Zalazar, C. S.; Labas, M. D.; Brandi, R. J.; Cassano, A. E. Dichloroacetic acid degradation employing hydrogen peroxide and UV radiation. *Chemosphere* **2007**, *66*, 808–815.

(33) Ollis, D. F.; Hsiao, C. Y.; Budiman, L.; Lee, C. L. Heterogeneous photoassisted catalysis: conversions of perchloroethylene, dichloroethane, chloroacitic acids, and chlorobenzenes. *J. Catal.* **1984**, *88*, 89–96.

(34) Czili, H.; Horváth, A. Photodegradation of chloroacetic acids over bare and silver-deposited TiO_2: Identification of species attacking model compounds, a mechanistic approach. *Appl. Catal., B* **2009**, *89*, 342−348.

Received for review April 19, 2009
Revised manuscript received August 22, 2009
Accepted August 31, 2009

IE900620N